J Low Temp Phys (2017) 189:120–131
DOI 10.1007/s10909-017-1794-y

Inhomogeneous Superconducting Behaviour in $La_5Ni_2Si_3$

M. Falkowski[1,2] · A. Kowalczyk[1] · A. M. Strydom[3] · M. Reiffers[4] · T. Toliński[1]

Received: 21 December 2016 / Accepted: 29 June 2017 / Published online: 12 July 2017

Abstract The superconducting phase transition at $T_c = 2.3\,\mathrm{K}$ was observed for the electrical resistivity $\rho(T)$ and magnetic susceptibility $\chi(T)$ measurements in the ternary compound $La_5Ni_2Si_3$ that crystallizes in the hexagonal-type structure. Although a single-phase character with the nominal stoichiometry of the synthesized sample was confirmed, a small trace of the La–Ni phase was found, being probably responsible for the superconducting behaviour in the investigated compound. The magnetization loop recorded at $T = 0.5\,\mathrm{K}$ resembles a star-like shape which indicates that the density of the critical current can be strongly suppressed by a magnetic field. The low-$T_\rho(T)$ and specific heat $C_p(T)$ data in the normal state reveal simple metallic behaviour. No clear evidence of a phase transition to any long- or short-range order was found for $C_p(T)$ measurements in the T-range of 0.4–300 K.

Keywords Superconductivity · Crystal structure · Magnetic properties · Electron transport · Thermodynamic properties

✉ M. Falkowski
falkowski@ifmpan.poznan.pl

1 Institute of Molecular Physics, Polish Academy of Sciences, Smoluchowskiego 17, 60-179 Poznan, Poland

2 Department of Condensed Matter Physics, Faculty of Mathematics and Physics, Charles University, Ke Karlovu 5, 12116 Prague 2, Czechia

3 Highly Correlated Matter Research Group, Physics Department, University of Johannesburg, PO Box 524, Auckland Park 2006, South Africa

4 Faculty of Humanities and Natural Sciences, University of Prešov, 17 Novembra 1, 081 16 Prešov, Slovakia

1 Introduction

Most often interesting physical properties, such as long-range magnetic order, heavy fermion behaviour, Kondo effect, intermediate valence behaviour or finally unconventional superconductivity, are attributed to the Ce-based compounds due to strong electronic correlations between the unfilled $4f$ shell and conduction band. The corresponding La compounds are also of interest as a reference systems due to the lack of the $4f$ electrons and that they crystallize usually in the same crystal structure as their Ce counterparts. Therefore, in recent years one can notice a growing interest in a study of La-based ternary alloys, which are superconductors at low temperatures. This group includes mostly intermetallic compounds, which crystallize in the skutterudite-type structure (e.g. $LaRu_4X_{12}$ (X = P, As and Sb) [1], LaT_4As_{12} (T = Fe, Ru and Os) [2] and $La_3T_4Sn_{12}$ (T = Co and Rh) [3]) and orthorhombic $U_3Ni_4Si_4$-type structure (*e.g.* $La_3Ni_4X_4$ (X = Si and Ge) and $La_3Pd_4Ge_4$ [4–6]). However, interesting examples of the ternary La-based superconducting compounds one can also find in the narrow group of alloys being the non-magnetic reference compounds for their highly correlated Ce-based counterparts. That applies, for example, to the two orthorhombic pairs of intermetallic systems, namely $(Ce, La)_3Rh_2Ge_2$, where $Ce_3Rh_2Ge_2$ is the antiferromagnetic dense Kondo compound [7], and (Ce, La)RhAl, where the $4f$ electron counterpart shows mixed valent behaviour of the cerium ions [8].

Among the ternary systems, there is also another interesting pair of intermetallics, namely $(Ce, La)_5Ni_2Si_3$, where $Ce_5Ni_2Si_3$ is a heavy fermion geometrically frustrated magnetic compound, whereas $La_5Ni_2Si_3$ is its non-magnetic analogue with superconducting transition at $T_c \simeq 1.8$ K [9]. $La_5Ni_2Si_3$ crystallizes in the hexagonal space group $P63/m$ of the $Ce_5Ni_2Si_3$ structure type (see Fig. 1), where each crystallographic site is fully occupied by a unique element [10]. In this structure, La atoms are located in four non-equivalent crystallographic positions, due to the different values of the atomic coordinates, while in the case of Ni and Si the atoms are, respectively, in three and two non-equivalent positions in the unit cell [10]. As far as could be ascertained, the comprehensive studies of superconducting properties have not yet been reported to date for $La_5Ni_2Si_3$. The only report indicating the occurrence of a superconducting transition in $La_5Ni_2Si_3$ was communicated by Lee et al. [9] based on the resistivity measurements. With this motivation, in this paper we report the results of X-ray diffraction, electrical resistivity as well as the low-temperature magnetization and specific heat measurements, but mainly we focus on the superconducting properties of $La_5Ni_2Si_3$.

2 Samples and Experiment

The polycrystalline sample of $La_5Ni_2Si_3$ was prepared by direct argon arc-melting of stoichiometric quantities of the elements in ultra-high purity argon with further in situ purification of argon. The purity for all reactant elements was 99.9 wt% or better. The specimen was remelted several times to ensure homogeneity, without significant weight loss confirmed to 0.3 wt%. Subsequently, the resulting alloy was annealed at 900 °C for 1 week in an evacuated quartz ampoule and finally quenched in cold water.

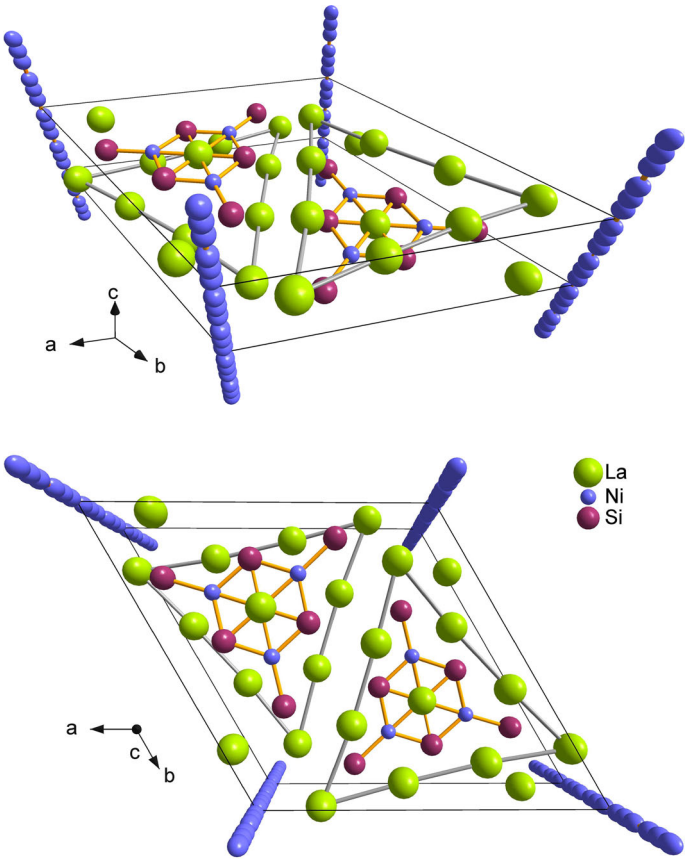

Fig. 1 Perspective view (*top*) and view along the *c*-axis of the unit cell of $La_5Ni_2Si_3$ (*bottom*) (Colour figure online)

Powder X-ray diffraction confirmed the single-phase nature of the investigated compound and showed straight-forward agreement with the expected crystal structure of the hexagonal $Ce_5Ni_2Si_3$-type structure with space group $P63/m$. Lattice parameters values for $La_5Ni_2Si_3$, $a = 16.2128(9)$Å and $c = 4.3495(5)$Å determined from full-profile spectra analysis with the FullProf software (see Fig. 2) are in close agreement with formerly reported values [10]. Additionally, the homogeneity and composition of the annealed sample were identified by the X-ray energy-dispersive microanalysis (EDX). The EDX investigation yielded the composition La: 51.7 at.%, Ni: 20.0 at.% and Si: 28.3 at.%, that corresponds to the formula $La_{5.2}Ni_{2.0}Si_{2.8}$, with a small deficiency of Si. From the obtained results, it can be stated that the quality of the prepared alloy is quite good, as for standards of the polycrystalline materials, with the estimated stoichiometry close in proximity to the expected. However, a close inspection of the EDX data of our sample also revealed additional contribution from the binary La–Ni phase at around few % despite the long heat treatment of the specimen (see Fig. 3). Physical properties were studied using a PPMS-9T and MPMS-7T sys-

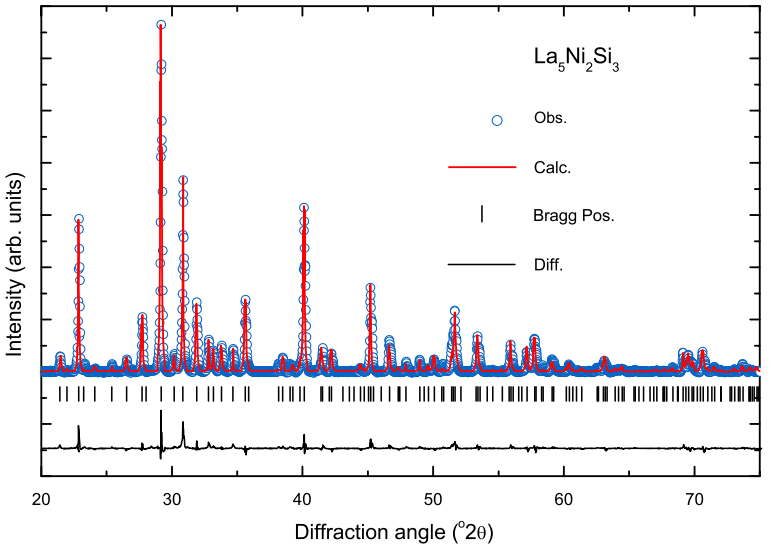

Fig. 2 Room temperature powder X-ray diffraction spectrum of $La_5Ni_2Si_3$. Experimentally observed intensities are indicated by the *circles*. The *red solid line* represents a full-profile Rietveld refinement using the FullProf software with the lattice parameters given in the text. The *vertical bars* index the hexagonal structure (space group $P63/m$). The difference between measured and calculated intensity is shown at the *bottom of the figure* (Colour figure online)

tem from *Quantum Design* equipped with low-temperature facilities including a ^{3}He recirculating insert. Electrical resistivity measurements were taken on a bar-shaped sample via a conventional four-probe technique. The estimated value of the material density for the studied specimen has been calculated based on the structural data using the FullProf software, yielding in approximation 5.72(2) g/cm^3.

3 Results and Discussion

Figure 4 (main panel) shows the zero-magnetic field temperature dependence of the electrical resistivity $\rho(T)$ of $La_5Ni_2Si_3$ measured in T-range of 0.4–300 K. As can be inferred from Fig. 4, at low temperatures between 2.5 and 25 K, $\rho(T)$ of $La_5Ni_2Si_3$ is characterized by a metallic behaviour together with the electron–phonon scattering as is apparent from the following equation [11]: $\rho(T) = \rho_0 + \rho_{\mathrm{el-el}}T^2 + \rho_{\mathrm{el-ph}}T^5$, where ρ_0 means the temperature-independent residual resistivity value, the electron–electron scattering in non-interacting Fermi gas leads to the quadratic term, whereas the electron–phonon scattering gives in the Bloch–Grüneisen approximation the T^5 contribution. With increasing temperature above ~50 K, the electrical resistivity does not behave like simple metals, revealing a significant deviation from the Bloch–Grüneisen–Mott (BGM) description [12]. Usually this pronounced curvature in $\rho(T)$ is observed for intermetallic compounds with transition metal elements and is connected with a strong interband s–d scattering of the conduction electrons [13]. On the other hand, a similar tendency in $\rho(T)$ was noticed for weakly correlated 3d and 5d

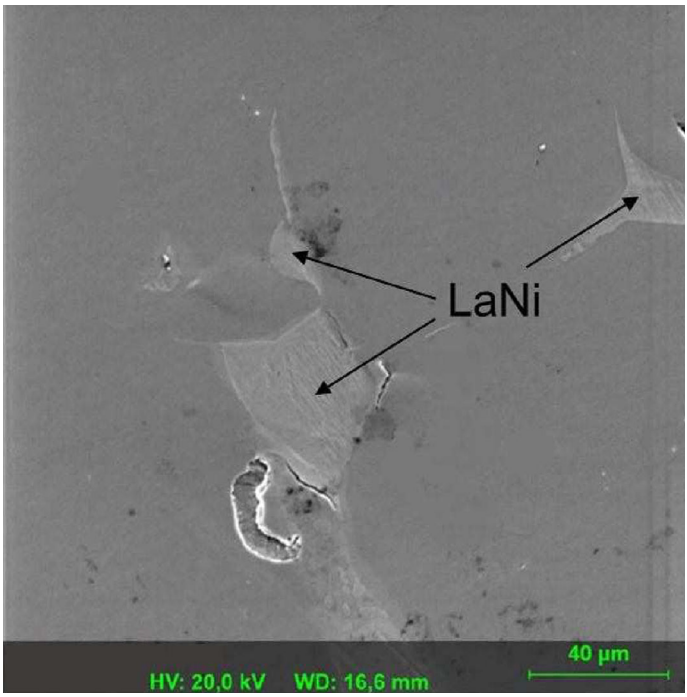

Fig. 3 Metallographic image of the microstructure of a polished surface of $La_5Ni_2Si_3$ obtained from the X-ray energy-dispersive microanalysis (EDX). The *light grey regions* pointed by *arrows* correspond to the LaNi binary phase (Colour figure online)

transition metals and high-T_C cuprates [14], as well as for mixed valent [15] and other highly correlated materials [16]. However, such significant departure from the BGM behaviour may be also attributed to a substantial electron–phonon interaction strength responsible for the formation of Cooper pairs in conventional superconductors. In order to properly describe the resistivity data in the normal state, we make use of a well-known model, the so-called parallel resistor model (PRM), which was predicted for characterizing $\rho(T)$ of A15-type superconductors [17]. This phenomenological model is based on the idea that the ideal resistivity must approach some limiting value in the regime where the mean free path becomes comparable to the interatomic spacing and is given by the following expression:

$$\rho(T) = \rho_0 + \frac{\rho_{\mathrm{ph}}(T) \cdot \rho_{\max}}{\rho_{\mathrm{ph}}(T) + \rho_{\max}} \tag{1}$$

where

$$\rho_{\mathrm{ph}}(T) = \rho_0 + \frac{4A_0}{\theta_R}\left(\frac{T}{\theta_R}\right)^n \int_0^{\theta_R/T} \frac{x^5 dx}{(e^x - 1)(1 - e^{-x})} \tag{2}$$

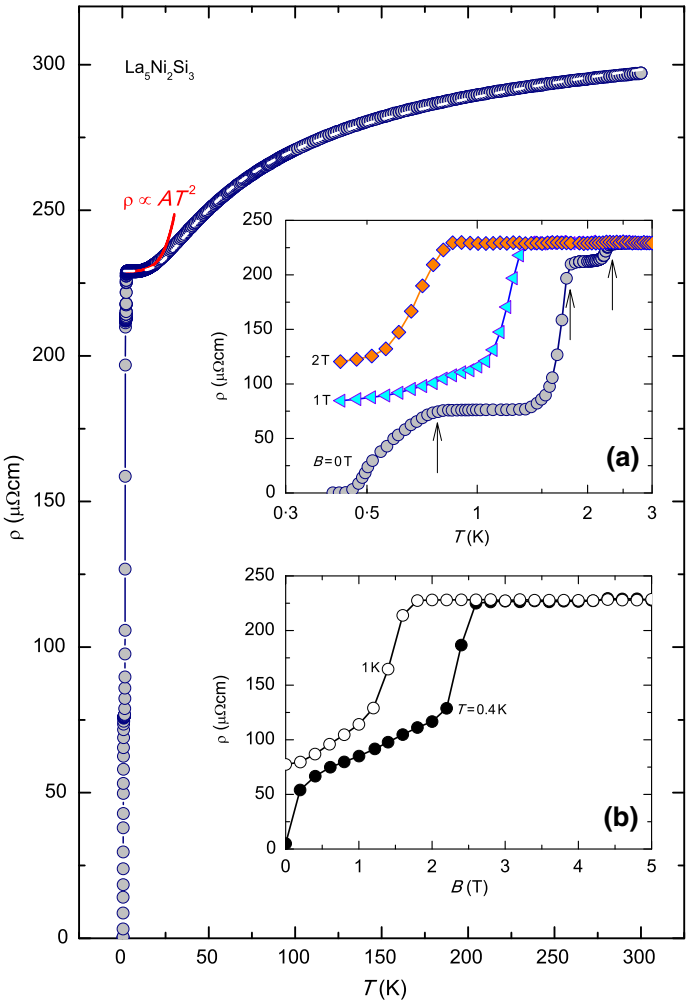

Fig. 4 Temperature dependence of the electrical resistivity of $La_5Ni_2Si_3$. The *dashed line* represents the fit of the parallel resistor model (Eq. 1) to the experimental data with parameters given in the text. *Inset* **a** shows low-T dependences of the electrical resistivity in vicinity of the superconducting transition in different applied magnetic fields. *Inset* **b** shows low-T magnetic field dependence of the electrical resistivity at constant temperatures (Colour figure online)

is the Bloch–Grüneisen function describing the phonon part of the resistivity and $\rho_{\max}$ denotes the saturation resistivity which is independent of the temperature. The applied fitting procedure by using Eq. (1) (see dashed line in main panel of Fig. 4) gives a satisfactory description of $\rho(T)$ in the normal state of $La_5Ni_2Si_3$ with the least-square (LSQ) fit parameters, which are as follows: $\rho_0 = 229\,\mu\Omega\,\mathrm{cm}$, $A_0 = 289.9\,\mu\Omega\,\mathrm{cm\,K}$, $\theta_R = 173\,\mathrm{K}$, $n = 4.4$ and $\rho_{\max} = 297\,\mu\Omega\,\mathrm{cm}$. The large value of the electron–phonon coupling parameter A_0 seems to confirm our suspicions for a substantial role of interactions between electrons and phonons at high temperatures in this compound. In the

Fermi liquid regime, $\rho(T)$ rapidly decreases with decrease in temperature down to 2.3 K, manifesting the onset of superconducting state. For the sake of clarity and in order to emphasize the low-T characteristic features, we show on the semilog scale the temperature behaviour of the electrical resistivity below 3 K under the absence and in an applied magnetic fields (see inset (a) in Fig. 4). Interestingly, instead of a sharp transition, which is characteristic for typical superconductors we have noticed that under zero-field $\rho(T)$ exhibits three step-like anomalies at 2.3, 1.8 and 0.77 K, until it reaches a clear limit of superconducting state, where $\rho(T) = 0$ at $T = 0.45$ K. Such behaviour is not commonly observed for conventional superconductors. A most likely cause of such behaviour seems to be connected with the presence of a trace of the La–Si phase. In the binary La–Si system, there are five intermetallic phases: La_5Si_3, La_5Si_4, La_3Si_2, $LaSi_2$ and LaSi [18]. Among these, the superconductivity was found in three tetragonal systems, $LaSi_2$ with α-$ThSi_2$ crystal structure ($T_c = 2.3$ K) [19], La_3Si_2 with U_3Si_2 crystal structure ($T_c \simeq 2.1$ K) [18,20] and La_5Si_3 with Cr_5B_3 crystal structure ($T_c = 1.6$ K) [18,21]. However, none of these superconducting La–Si phases was detected through electron microprobe analysis in our sample. Instead, we have detected via EDX analysis a small trace of the LaNi phase (see Fig. 3), undetectable from the X-ray data and most probably responsible for appearing of the superconductivity in our sample. In the case of the superconducting binary La–Ni phases, one can mention of two compounds, namely La_7Ni_3 with the hexagonal Th_7Fe_3 type crystal structure ($T_c = 2.1$ K) [22,23] and La_3Ni with the orthorhombic Fe_3C type crystal structure ($T_c \simeq 1.45$ K) [24]. It must also be recalled that superconductivity in Ni containing compounds is rather rare due to the strong magnetic character of Ni atoms that might break the Cooper pairs and destroy superconductivity. Therefore, if the superconductivity appears in such systems it usually has unconventional or more exactly saying inhomogeneous character. An interesting example can constitute here the Ni based ternary carbide compound $LaNiC_2$, which crystallizes in the orthorhombic $CeNiC_2$ type structure ($T_c = 2.7$ K), where the deviations from conventional BCS behaviour have been interpreted as evidence for triplet superconductivity [25,26]. On the other hand, it should be noted here that the superconducting behaviour in $La_5Ni_2Si_3$ may originate from the other reason, namely from the coexistence of the superconducting phase and magnetic correlations. At this point, it is pertinent to note that the 4f electron counterpart $Ce_5Ni_2Si_3$ is a geometrically frustrated magnet with $T_N \simeq 5.7$–7.3 K [9,27,28]. The long-range magnetic order below T_N is characterized by competing interactions between Ce ions, where the magnetic moments are strongly frustrated. From the low-T measurements of the magnetic susceptibility for the $Ce_{5-x}La_xNi_2Si_3$ system, it has turned out that for $x \leq 2$ the anomaly due to an antiferromagnetic ordering is still observed [29]. Nevertheless, we have not found the unambiguous evidence for the existence of any magnetic correlations in $La_5Ni_2Si_3$ based on $C_p(T)$ measurements in T-range of 0.4–300 K (not shown here).

The application of a moderate magnetic field gradually suppresses superconductivity of $La_5Ni_2Si_3$. Inset (b) in Fig. 4 shows a field dependence of resistivity measured at $T = 0.4$ and 1 K. As can be seen, upon increasing a magnetic field the '*pure*' superconductivity at $T = 0.4$ K vanishes already in very low fields; however, the overall superconducting transition gets suppressed in the field above $B = 2.6$ T. The residual resistivity ratio (RRR) = $\rho(300\text{ K})/\rho(2.5\text{ K})$ of $La_5Ni_2Si_3$ amounts to 1.3. This low

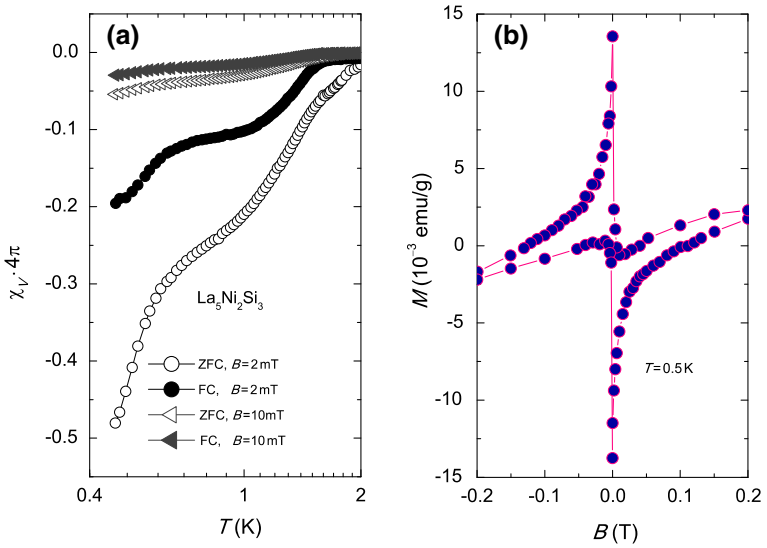

Fig. 5 **a** Low-temperature ZFC and FC dependences of the volume susceptibility measured below 2 K in different magnetic fields. **b** The magnetization hysteresis loop of $La_5Ni_2Si_3$ recorded at $T = 0.5$ K (Colour figure online)

value of RRR is in line with large value of ρ_0, thereby indicating on the substantial amount of the atomic disorder, the grain boundary effect or the existence of other structural defects in the investigated polycrystalline sample.

The low-T magnetic properties of $La_5Ni_2Si_3$ are depicted in Fig. 5a, b. Figure 5a shows the normalized temperature dependence of the volume susceptibility $\chi_V(T)$ measured in zero-field cooling (ZFC) and field cooling (FC) conditions in the magnetic fields of 2 and 10 mT. Below $T = 2$ K, $\chi_V(T)$ of $La_5Ni_2Si_3$ significantly decreases with a predominant role of diamagnetic screening signal due to the Meissner–Ochsenfeld effect in the superconducting state. As displayed in Fig. 5a, the ZFC and FC curves differ in their magnitude ($\sim$60%) at $T = 0.45$ K in low applied magnetic field of 2 mT. This behaviour proves the substantial role of the flux pinning in the FC mode, which usually occurs in the bulk polycrystalline metallic superconductors having a weak flux exclusion fraction [30,31]. With rising magnetic field strength, the diamagnetic signal in $La_5Ni_2Si_3$ becomes suppressed and superconductivity gradually vanishes. In relation to $\rho(T)$ data, one can draw a similar conclusion, namely the absence of a sharp superconducting transition and the lack of saturation of the susceptibility in the lowest temperatures. This might result from an intrinsic mechanism, such as competition between the superconductivity and strong magnetic character of Ni atoms in this compound, or it could suggest that despite the large diamagnetic signal the superconductivity is confined to small fractions of the sample. As can be seen in Fig. 5a, the percentage amount of the theoretical value of $-1/4\pi$ expected for a perfect shielding of the total volume of the sample, estimated at 0.45 K in the ZFC regime and $B = 2$ mT reaches $\sim$48%. The field dependence of magnetization $M(B)$ at constant temperature $T = 0.5$ K is shown in Fig. 5b. The visible hysteresis loop clearly

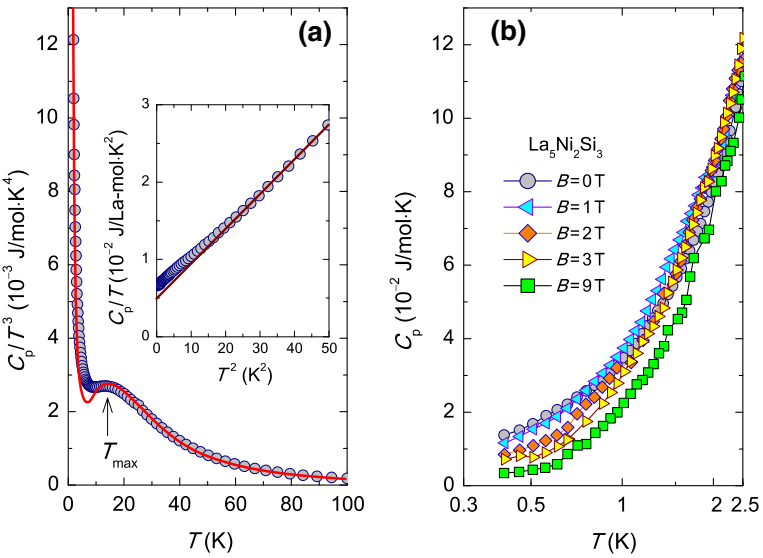

Fig. 6 **a** Temperature dependence of the ratio $C_p(T)/T^3$ with a fit of the data by using Eq. 3 (see *red solid line*) and the parameters given in the text. *Inset* illustrates a plot of $C_p(T)/T$ versus T^2 and a fit of the electronic specific heat. **b** Low-temperature specific heat data in the applied magnetic fields (Colour figure online)

exhibits a behaviour characteristic of type-II superconductor. We have found that the hysteresis loop is very narrow, and its irreversible behaviour disappears rapidly with the applied magnetic field. Such tendency indicates that the critical current is strongly field dependent and that the flux pinning exists only in the low range of the magnetic field.

With reference to the crystal structure and high-T variation of the electrical resistivity, where $\rho(T)$ significantly deviates from the BGM behaviour, we may expect that the enhanced phonon contribution is probably derived from the anharmonic vibrations of the La ions. This assumption seems to be justified in the context of the specific heat data displayed in the form $C_p(T)/T^3$ versus T (see Fig. 6a) to assess the presence of low-frequency anharmonic vibrational Einstein modes. One should observe the occurrence of a maximum at $T = T_{max}$. As can be inferred from Fig. 6a, a small maximum occurs at T_{max} = 14 K. The description of the specific heat data in terms of a combination of acoustic and optic vibrational modes can readily be associated with the crystal structure properties of $La_5Ni_2Si_3$, because every filled atomic site in the unit cell is occupied by only one element. In our analysis, the specific heat data between $2 < T < 100$ K can be treated as the sum of a phononic and an electronic contribution. The electronic specific heat coefficient γ was estimated from a linear fit to $C_p(T)/T$ versus T^2 for $T < 7$ K (see inset in Fig. 6a) yielding the value $\gamma = 6.5$ mJ/La-mol K^2, which confirms a metallic behaviour of $La_5Ni_2Si_3$. However, the value of γ coefficient of $La_5Ni_2Si_3$ is somewhat enhanced compared to the typical ordinary metals. In $La_5Ni_2Si_3$, owing to the absence of 4f-electrons, the electron–electron correlations are not anticipated to be very strong, and therefore, this issue seems to be quite intriguing.

In Fermi liquids, it is widely known that the T^2-coefficient of the electrical resistivity $\rho_{\mathrm{el-el}}$ is proportional to the square of the electronic specific heat coefficient γ^2 [32]. Using the values $\rho_{\mathrm{el-el}} = 0.0033\,\mu\Omega\,\mathrm{cm/K^2}$ and $\gamma = 6.5\,\mathrm{mJ/La\text{-}mol\,K^2}$, we obtain the Kadowaki–Woods ratio $\rho_{\mathrm{el-el}}/\gamma^2 = 7.8 \times 10^{-5}\,\mu\Omega\mathrm{cm\,La\text{-}mol^2\,K^2/mJ^2}$. It should be noted that the estimated value of the Kadowaki–Woods ratio of $La_5Ni_2Si_3$ is slightly larger to that of the Fermi liquid systems $\rho_{\mathrm{el-el}}/\gamma^2 \simeq 1.0 \times 10^{-5}\,\mu\Omega\,\mathrm{cm\,mol^2\,K^2/mJ^2}$ [32]. The red solid line superimposed on $C_{\mathrm{p}}(T)/T^3$ versus T represents the LSQ fit using the combined Debye and Einstein vibrational modes given by:

$$C_{\mathrm{p}}(T) = \gamma T + \frac{9R}{1-\alpha_D T}\left(\frac{T}{\theta_D}\right)^3 \int_0^{\theta_D/T} \frac{x^4 e^x \mathrm{d}x}{(e^x-1)^2} + R\sum_{i=1}^{27} \frac{1}{1-\alpha_E T}\left(\frac{\theta_E}{T}\right)^2 \frac{e^{\theta_E/T}}{(e^{\theta_E/T}-1)^2} \tag{3}$$

yielding the following values of parameters: $\theta_D = 212\,\mathrm{K}$, $\theta_{E1} = 77\,\mathrm{K}$, $\theta_{E2} = 125\,\mathrm{K}$, $\theta_{E3} = 286\,\mathrm{K}$ and $\alpha_D = 10\times10^{-5}$, $\alpha_{E1} = 12\times10^{-5}$, $\alpha_{E2} = 10\times10^{-5}$, $\alpha_{E3} = 11\times10^{-5}$, where θ_D and θ_E are the characteristic Debye and Einstein temperatures of the acoustic and optical branches. Additionally, all phonon branches were corrected by anharmonicity coefficients α_D and α_E due to a small but not negligible contribution to the phonon spectrum at high temperatures [33].

Specific heat measurements down to 0.4 K have not revealed a clear anomaly associated with the superconducting transition. The absence of the specific heat jump in the zero-field $C_{\mathrm{p}}(T)$ data, which is a characteristic feature of the bulk superconductors, as it is foreseen in the framework of the BCS theory, suggests that the superconductivity in $La_5Ni_2Si_3$ has non-bulk character and arises from a superconducting impurity phase. Figure 6b shows the low-T specific heat data measured between 0.4 and 2.5 K in applied fields of 0, 1, 2, 3 and 9 T. The overall temperature dependence of $C_{\mathrm{p}}(T)$ below 2.5 K shows a behaviour that is rather characteristic of a well-behaved metal.

4 Conclusions

The polycrystalline $La_5Ni_2Si_3$ sample was synthesized in order to check its superconducting properties. Based on the measurements of $\rho(T)$ and $\chi(T)$, we have found that $La_5Ni_2Si_3$ undergoes a superconducting phase transition below $T_{\mathrm{c}} = 2.3$ K. Our results are in agreement with the previous observations of Lee et al. [9] who noticed the appearance of a superconducting transition in $\rho(T)$ at about 1.8 K. We have found that the investigated compound behaves as a type-II superconductor. The occurrence of three step-like transitions in the resistivity at 2.3, 1.8 and 0.77 K, before $\rho(T)$ reaches a clear limit of superconducting state at 0.45 K, and lack of the characteristic specific heat jump in the zero-field $C_{\mathrm{p}}(T)$ data imply that the superconductivity in the investigated compound is inhomogeneous and is rather a consequence of the spurious contribution from a trace of the binary La–Ni phase. However, apart from that conclusion we should also consider an alternative option, namely the contribution of the structural factor in context of the complexity of the crystal structure, where each crys-

tallographic site is fully occupied by a unique element and, moreover, La atoms are located in four non-equivalent positions. The low-temperature $\rho(T)$ and $C_p(T)$ data in the normal state consistently suggest that a ground state of $La_5Ni_2Si_3$ is metallic.

Acknowledgements MR thanks the University Science Park TECHNICOM for Innovation Applications Supported by Knowledge Technology, ITMS: 26220220182, supported by the Research and Development Operational Programme funded by the ERDF. AMS thanks the FRC/URC of the University of Johannesburg and the SA-NRF (93549) for financial assistance. Barbora Vondráčková is thanked for the EDX measurement assistance.

References

1. T. Uchiumi, I. Shirotani, Ch. Sekine, S. Todo, T. Yagi, Y. Nakazawa, K. Kanoda, J. Phys. Chem. Sol. **60**, 689 (1999)
2. I. Shirotani, K. Ohno, Ch. Sekine, T. Yagi, T. Kawakami, T. Nakanishi, H. Takahashi, J. Tang, A. Matsushita, T. Matsumoto, Physica B **281–282**, 1021 (2000)
3. A. Ślebarski, M. Fijałkowski, M.M. Maśka, M. Mierzejewski, B.D. White, M.B. Maple, Phys. Rev. B **89**, 125111 (2014)
4. H. Fujii, J. Phys. Condens. Matter **18**, 8037 (2006)
5. H. Fujii, S. Kasahara, J. Phys. Condens. Matter **20**, 075202 (2008)
6. S. Kasahara, H. Fujii, H. Takeya, T. Mochiku, A.D. Thakur, K. Hirata, J. Phys. Condens. Matter **20**, 385204 (2008)
7. D. Kaczorowski, Yu. Prots, Yu. Grin, Phys. Rev. B **64**, 224420 (2001)
8. N.H. Kumar, S.K. Malik, Phys. Rev. B **62**, 127 (2000)
9. B.K. Lee, D.H. Ryu, D.Y. Kim, J.B. Hong, M.H. Jung, H. Kitazawa, O. Suzuki, S. Kimura, Y.S. Kwon, Phys. Rev. B **70**, 224409 (2004)
10. Y.M. Prots, W. Jeitschko, Inorg. Chem. **37**, 5431 (1998)
11. G. Grimvall, *The Electron–Phonon Interaction in Metals* (North-Holland, Amsterdam, 1981)
12. N.F. Mott, H. Jones, *The Theory of the Properties of Metals and Alloys* (Oxford University Press, London, 1958)
13. N.F. Mott, Proc. R. Soc. A **153**, 699 (1935)
14. O. Gunnarsson, M. Calandra, J.E. Han, Rev. Mod. Phys. **75**, 1085 (2003)
15. J. Goraus, A. Ślebarski, M. Fijałkowski, J. Alloys Compd. **509**, 3735 (2011)
16. C.S. Sunandana, Ed. L.C. Gupta, S.K. Malik, Theoretical and Experimental Aspects of Valence Fluctuations and Heavy Fermions: Electrical Behaviour of Heavy Electron Compounds. Plenum, New York, p 421 (1987)
17. H. Wiesmann, M. Gurwitch, H. Lutz, A.K. Ghosh, B. Schwarz, M. Strongin, P.B. Allen, J.W. Halley, Phys. Rev. Lett. **38**, 782 (1977)
18. M.V. Bulanova, P.N. Zheltov, K.A. Meleshevich, P.A. Saltykov, G. Effenberg, J.-C. Tedenac, J. Alloys Compd. **329**, 214 (2001)
19. T. Satoh, Y. Asada, J. Phys. Soc. Jpn. **28**, 263 (1970)
20. S.K. Dhar, P. Manfrinetti, A. Palenzona, Y. Kimura, M. Kozaki, Y. Onuki, T. Takeuchi, Physica B **271**, 150 (1999)
21. J.L. Jorda, *La Based Alloys and Compounds (Materials—The Landolt–Börnstein Database)* (Springer, Berlin, 1990)
22. G.L. Olcese, J. Less Common Metals **33**, 71 (1973)
23. K. Umeo, K. Ishii, H. Kadomatsu, Solid State Commun. **90**, 321 (1994)
24. W.H. Lee, H.K. Zeng, Y.D. Yao, Y.Y. Chen, Physica C **266**, 138 (1996)
25. N. Sato, N. Koga, K. Imamura, T. Sakon, T. Komatsubara, Physica B **206–207**, 565 (1995)
26. V.K. Pecharsky, L.L. Miller, K.A. Gschneidner, Phys. Rev. B **58**, 497 (1998)

27. A. Kowalczyk, M. Falkowski, T. Toliński, Solid State Sci. **14**, 1496 (2012)
28. M. Mihalik, S. Mataš, J. Kováč, V. Kavečanský, M. Mihalik, P. Svoboda, Physica B **378–380**, 851 (2006)
29. B.K. Lee, H.J. Im, M.H. Jung, Y.S. Kwon, Physica B **403**, 1450 (2008)
30. Y. Takano, H. Takeya, H. Fujii, H. Kumakura, T. Hatano, K. Togano, H. Kito, H. Ihara, Appl. Phys. Lett. **78**, 2914 (2001)
31. K. Togano, P. Badica, Y. Nakamori, S. Orimo, H. Takeya, K. Hirata, Phys. Rev. Lett. **93**, 247004 (2004)
32. K. Kadowaki, S.B. Woods, Solid State Commun. **58**, 507 (1986)
33. C.A. Martin, J. Phys. Condens. Matter **3**, 5967 (1991)